Tr. J. of Physics
23 (1999) , 479 – 484.

The Lattice Dynamics of γ-Iron

K. ÇOLAKOĞLU, G. UĞUR, M. ÇAKMAK, H. M. TÜTÜNCÜ
Gazi University, Faculty of Arts and Sciences,
Ankara-TURKEY

Received 21.02.1997

Abstract

Lattice dynamical calculations are performed on γ-iron using the Clark-Gazis-Wallis (CGW) model to represent the ion-ion interactions, and a modified form of the Sharma-Joshi model to include ion-electron interactions. The theory is used to compute the phonon dispersion curves, frequency spectra and the lattice specific heat of γ-iron. The obtained results are in good agreement with the experimental findings, and are better than those calculated using the other theories.

Introduction

As is well known, iron is bcc α-phase at low temperature and it undergoes tranformation to the fcc γ-phase at approximately 1200K, then transforms to bcc δ-phase at approximately 1670K. Because of its technological importance, many papers exist in the literature on the lattice dynamics of bcc iron [1-4], but fewer investigations are published for γ-iron [5,6,7], the reason being the difficulty of growing *in situ* single crystals for γ-iron. After Zarestky and Stassis measurement [8] of γ-iron phonon frequencies at high temperature the present work is the fourth theoretical study on the lattice dynamics of γ-iron.

Okoye and Pal [7] computed the phonon frequencies of γ-Fe within the frame work of the transition metal model potential (TMMP) approach of Animalu [9], including the contribution of the short-range three-body interactions. Since the d-electrons and the conduction electrons present in the transition metals significantly affect the lattice dynamical behavior in γ-iron, the TMMP approach does not give very good agreement with experiments (mainly for the trasverse modes of vibration) and thus is limited as a model. Moreover, transition metals pseudopotential and second-order pertubation theories are also inadequate and unsatisfactory for γ-iron [7].

Singh and Rathore [6], approached the problem using a pairwise potential giving higher frequencies than those of experiment, mainly in the longitudinal branches. Al-

though the pairwise potential produces the same dynamical matrix as those of the DAF (de Launay Angular Force) model [10,11,12], its dynamical matrix is not rotationlaly invariant [11].

In this paper, we have used the CGW angular force model, developed orginally by Clark-Gazis-Wallis [2], and have included ion-electron interactions following the scheme of Behari and Tripathi [13,14,15]. The CGW model guarantes rotational invariance for the resulting dynamical matrix [11,16,17], and gives a dynamical matrix different from the DAF model for fcc metals [18].

Theory and Computation

Secular Determinant

The phonon frequencies in the harmonic approximation are given by the usual secular equation

$$|D_{\alpha\beta}(\vec{k}) - m\omega^2 I\delta_{\alpha\beta}| = 0, \tag{1}$$

where

$$D_{\alpha\beta}(\vec{k}) = D^{i-i}_{\alpha\beta}(\vec{k}) + D^{i-e}_{\alpha\beta}(\vec{k}). \tag{2}$$

Here, $D_{\alpha\beta}(\vec{k})$ are the elements of the dynamical matrix, $(\vec{k})$ is the wave vector confined to the first Brillouin zone, I is the unit matrix of order three and m is the ionic mass. In this present scheme the ion-ion interaction $D^{i-i}_{\alpha\beta}(\vec{k})$ is represented by the CGW model, which is effective up to second neighbours, and the ion-electron interaction $D^{i-e}_{\alpha\beta}(\vec{k})$ is assumed to have the form of the Behari and Tripathi model [15].

The elements of the dynamical matrix in Eq.(1) for fcc structure are given by Bose *et al.* [18]:

$$\begin{aligned} D_{xx} = {} & 2\left[\alpha + \frac{8}{a^2}(\gamma_1+\gamma_2)\right][2 - C_1(C_2+C_3)] + 4\beta S_1^2 \\ & - \frac{4\gamma_1}{a^2}(2\cos 2\pi a k_1 - \cos 2\pi a k_2 - \cos 2\pi a k_3) \\ & + a^3\pi^2 k_1^2 k_e G^2(x) \end{aligned} \tag{3}$$

$$D_{xy} = 2\left(2\alpha - \frac{16\gamma_1}{a^2}\right) S_1 S_2 + a^3\pi^2 k_1 k_2 k_e G^2(x), \tag{4}$$

where $C_i = \cos \pi a k_i, S_i = \sin \pi a k_i, G(x) = 3(\frac{\sin x - x\cos x}{x^3})$ and $x = 2\pi k\gamma_0.\alpha, \beta$ and γ_1, γ_2 are the central and angular force constants corresponding to the first and second neighbours, respectively. a, k_i, γ_0 and k_e are the lattice constant, the phonon wave vector compenents, the radius of the Wigner-Seitz sphere and the bulk modulus of the electron

gas, respectively.

Force Constants

By expanding the secular determinant in the long-wavelength limit ($k \to 0$), one gets the following relations between the elastic constants and the force constants, as in [18]:

$$\begin{aligned} aC_{11} &= 2\alpha + 2\beta + \frac{32\gamma_1}{a^2} + \frac{16\gamma_2}{a^2} + ak_e \\ aC_{12} &= \alpha - \frac{16\gamma_1}{a^2} - \frac{8\gamma_2}{a^2} + ak_e \\ aC_{44} &= \alpha + \frac{8\gamma_2}{a^2} \\ m\omega_L^2 &= 8\alpha + \frac{64\gamma_1}{a^2} + \frac{64\gamma^2}{a^2} + ak_e\pi^2 G^2(x) \\ m\omega_T^2 &= 4\alpha + \frac{32\gamma_1}{a^2} + \frac{32\gamma^2}{a^2}, \end{aligned} \tag{5}$$

where C_{11}, C_{12} and C_{44} are measured elastic constants; and $\nu_L (= \omega_L/2\pi)$ and $\nu_T (= \omega_T/2\pi)$ are the zone boundary frequencies in [100] direction.

Solutions to Eq (5) give the unknown constants, which are substituted in the dynamical matrix to find the phonon frequencies in he main symmetry directions [100], [110] and [111]. For the present work, the required experimental constants and the calculated parameters are given in Table 1 and Table 2, respectively.

Table 1. Input data [8,19] for computation of force constants.

C_{11} $10^{12}dyn/cm^2$	C_{12} $10^{12}dyn/cm^2$	C_{12} $10^{12}dyn/cm^2$	ν_L $10^{12}Hz$	ν_T $10^{-10}m$	a
1.54	1.22	0.77	7.4611	5.3867	3.64

Table 2. The calculated force constants for γ-iron in units of dyn/cm^2.

γ_1/a^2	γ_1/a^2	α	β	ak_e
-175.192	-936.955	35523.650	1755.136	-1414.378

The obtained force constants are then used to calculate the frequency distribution function, $g(\nu)$, as a function of frequency with the algorithm of Gilat and Raubenheimer [20] and is shown in Fig. 1. It shows very similar trends to that of Zarestky and Stassis's [8] calculations based on the experimental findings. Further, we have also computed the specific heat C_v at different temperatures from the formula [21]

$$C_v = \frac{3R}{3000} \sum_v E(hv/kT) g(\nu), \tag{6}$$

where $g(\nu)$ is the frequency distribution function for γ-iron, R the gas constant, and $E(h\nu/kT)$ the Einstein function defined by

$$E(x) = \frac{x^2 e^x}{(e^x - 1)^2}, \tag{7}$$

where $x = h\nu/kT$.

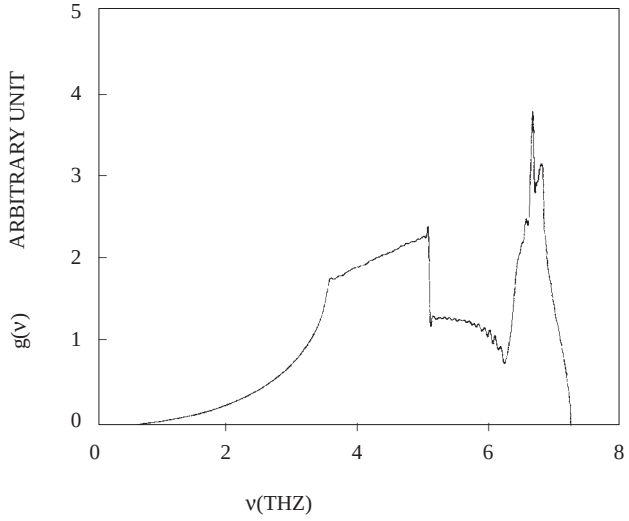

Figure 1. Phonon dispersion curves for γ-iron.

Numerical Results and Discussion

In order to determine the phonon frequencies of γ-iron, we have calculated the ion-ion and ion-electron interaction parts of the dynamical matrix following exactly the procedures in [15,18]. The computed dispersion curves for γ-iron are shown in Fig.2. The experimental values reported by Stassis [8] are also marked in the figure. A close inspection of the figure reveals that the computed curves are in good agreement with the experimental ones in all three symmetry directions except on the zone boundary in the [111] direction. The calculated frequencies in this direction are higher by about of %20 than those measured experimentally. The calculated maximum frequency for γ-iron is about of 7.26×10^{12}Thz, and is in good agreement with that derived from the experimental frequency distributions (7.26×10^{12}Thz). The temperature dependence of specific heat C_v is shown in Fig.3., and it shows the expected behaviour in low ($\theta \leq 10/T$) and high temperature values.

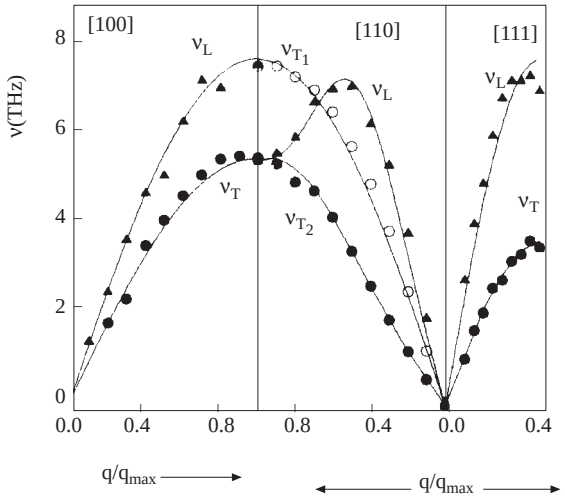

Figure 2. Frequency distribution curve of γ-iron.

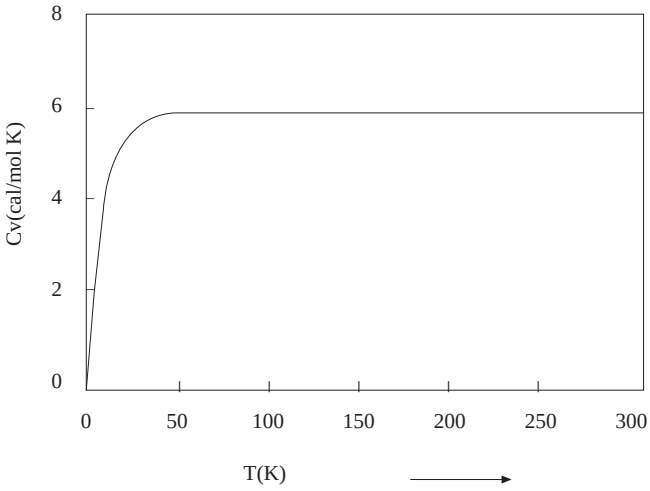

Figure 3. C_v-T curve for γ-iron.

It may be concluded that the present model represents correctly the actual interactions responsible for the lattice vibrations in γ-iron.

Acknowledgements

We wish to thank Professor Ş. Ellialtıoğlu for many helpful discussions on the frequency distribution function algorithm.

References

[1] A. O. E. Animalu, Phys. Rev. B, **8** (1973) 3555.

[2] B. C. Clark, D. C. Gazis, R. F. Wallis, Phys. Rev., **134** (1964) 1486.

[3] B. N. Brockhouse, H. E. Abou-Helal, and E. D. Hallman, Solid State Commun., **5** (1967) 211.

[4] M. W. Finnis and K. L. Kear, Phys. Rev. Lett., **52** (1984) 291.

[5] N. Singh, Phys. Stat. Sol.(b), **K33** (1989) 156.

[6] D. Singh, and R. P. S. Rathore, Phys. Stat. Sol.(b), **170** (1992) 443.

[7] C. M. I. Okoye, and S. Pal, Physica B, **183** (1993) 279.

[8] J. Zarestky, and C. Stassis, Phys. Rev. B, bf 35 (1987) 4500.

[9] A. O. E. Animalu, Phys. Rev. R, **8** (1973) 3542.

[10] J. DeLaunay, in Solid State Physics, Edited by F. Seitz and D. Turnbull (Academic Press Inc, New York, 1956), Vol 2, pp 219-303.

[11] Y. P. Varshini, and P. S. Yuen, Phys. Rev., **174** (1968) 7660.

[12] J. C. Upadhyaya, S. Lehri, D. K. Sharma, and S. C. Upadhyaya, Phys. Stat. Sol.(b), **59** (1990) 659.

[13] P. K. Sharma, and S. K. Joshi, J. Chem. Phys., **39** (1963) 2633.

[14] J. Behari, and B. B. Tripathi, Aus. J. Phys., **23** (1970) 311.

[15] J. Behari, and B. B. Tripathi, J. Phys. C: Solid State Phys., **3** (1970) 659.

[16] P. S. Yuen, and Y. P. Varshini, Phys. Rev., **164** (1967) 895.

[17] J. C. Upadhyaya, J. Phys. F: Metal Phys., **7** (1977) 769.

[18] G. Bose, H. C. Gupta, and B. B. Tripathi, J. Phys. F: Metal Phys., **2** (1972) 426.

[19] C. Kittel, Introduction to Solid State Physics (5-th ed., John Wiley, New York 1976).

[20] G. Gilat, L. J. Raubenheimer, Phys. Rev., **144** (1966) 390.

[21] V. K. Thakur, Phys. Stat. Sol.(b), **135** (1986) 67.